

# Helical Crimp Model Predicts Material Properties From Tendon Microstructure

Ann K. Harvey<sup>1</sup>  
harvey@robots.ox.ac.uk

Mark S. Thompson<sup>2</sup>  
mark.thompson@eng.ox.ac.uk

Sir Michael Brady<sup>1</sup>  
jmb@robots.ox.ac.uk

<sup>1</sup> Wolfson Medical Vision Laboratory  
Department of Engineering Science  
University of Oxford, Oxford, UK

<sup>2</sup> Institute of Biomedical Engineering  
Department of Engineering Science  
University of Oxford, Oxford, UK

---

## Abstract

The structural organisation at various levels of the tendon hierarchy is important for determining its biomechanical, functional, properties. The intricacies of this organisation, however, are not yet well defined. Developing tendon imaging and concurrent analysis methods are essential for exploring the clinical potential of image-based tendon assessment. This paper demonstrates a multimodal imaging approach for characterising tendon tissue at multiple spatial scales; high field magnetic resonance imaging and microscopy both distinguish between normal and damaged tendon, at different spatial scales. A multiple cylindrical helix model, which accounts for a range of observed crimp architectures, is proposed for interpreting images of normal and damaged tendon microstructure. Image-derived parameters, helix radius and pitch, are fitted to a mechanical helix model to predict changes in material property from tendon structure. Biomechanical insight suggests that abnormal fibre organisation increases tendon stiffness.

## 1 Introduction

Tendon injuries and disorders are becoming a major concern associated with daily activities, recreational and competitive sports. Estimated as accounting for 30-50% of all sports injuries, over-use injuries such as tendinitis are the most frequent cause of enforced breaks from activity [4]. As such, there is a growing demand for methods which can determine tendon tissue quality *in vivo*, such as magnetic resonance imaging (MRI) and endoscopic microscopy [5], for diagnostic and/or monitoring repair purposes. However, relatively little is known about the imaging correlates of healthy and abnormal tendon tissue, thus highlighting the current limitations associated with image-based tendon tissue quality assessment. In order to develop *in vivo* imaging methods, pre-clinical *ex vivo* investigation is required to determine the physiological source of signals in tendon MR and microscopy images, the physiological relationships between image-derived microstructure and function.

Tendon is a musculoskeletal tissue which transfers the forces generated by muscles to bones, by distributing loads between its multicomposite structure across multiple scales. From tropocollagen through to the macroscopic tendon *via* fibrils, fibres and fascicles, the cylindrical subunits are aligned predominantly along the longitudinal tendon axis (*i.e.* the

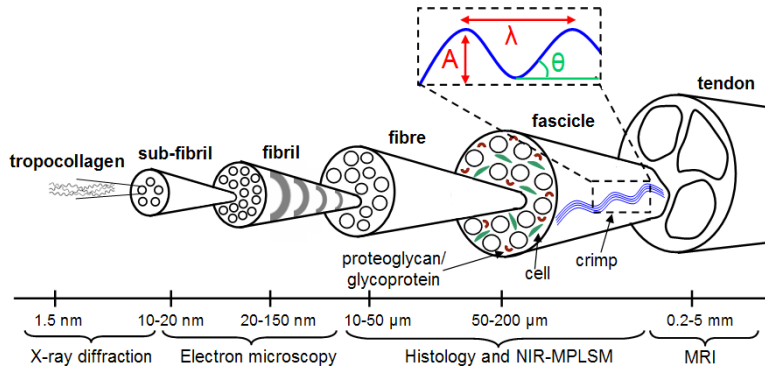


Figure 1: Tendon hierarchy and appropriate methods for investigating tendon tissue. Within fascicles, crimp is defined by crimp amplitude ( $A$ ), wavelength ( $\lambda$ ), and angle ( $\theta$ ).

primary loading direction) within a distinct hierarchy (Figure 1). The extracellular matrix (ECM) *composition, organisation* and *interactions* at different levels of the hierarchy govern the tendon material properties [7], and account for its nonlinear viscoelastic behaviours [1]. This paper demonstrates that the ECM organisation, captured by multimodal imaging, can reveal tendon properties related to tissue function.

Appropriate imaging methods are required to investigate the ECM organisation at different levels of the tendon hierarchy (Figure 1). Signal intensity relating to fascicular banding is captured by high field MRI, with  $\sim 0.5 \text{ mm}^2$  resolution [6]. Within fascicles, higher resolution ( $\sim 1 \mu\text{m}^2$ ) microscopy methods reveal the ECM organisation underlying the tissue morphology. In particular, near infrared multiphoton laser scanning microscopy (NIR-MPLSM) exploits the abundance of collagen in tendon fibrils to generate images, *via* second harmonic generation (SHG), of intrinsic fibre organisation. SHG images reveal crimp (Figure 1), a characteristic microscopic feature of tendon, linked to tendon nonlinear viscoelastic low strain behaviour ( $< 4\%$ ) *via* the straightening-out of crimped fibres [2, 7]. Although crimp architecture has not yet been resolved as 2D planar (zig-zag or sinusoidal) or 3D helical [2], crimp is typically defined (Figure 1) by the crimp angle ( $\psi = 5^\circ - 30^\circ$ ), or the crimp amplitude ( $A = 1 \mu\text{m} - 10 \mu\text{m}$ ) and crimp wavelength ( $\lambda = 10 \mu\text{m} - 100 \mu\text{m}$ ) [2]. Deviation from the expected values for a particular tendon and species is considered abnormal.

Tendon images are difficult to interpret because they are noisy, contain information at multiple scales, and inherently represent a 3D microstructure. From qualitative SHG image analysis, we observed viewpoint invariance over an angular range of tendon microstructure, more specifically crimp. Based on these observations, we propose a 3D helical model to facilitate tendon image analysis and interpretation, by adopting prior knowledge of tendon microstructure, and enabling biomechanical insight. This paper applies a multimodal imaging approach for characterising normal and damaged (experimentally-induced by enzyme-digestion) bovine tendon *ex vivo*. It offers image interpretation at multiple scales, relating to the underlying physiological subunits. Section 2 proposes a multiple cylindrical helix model that accounts for the observed crimp viewpoint invariance. Section 3 compares MR images, SHG images, and extracted crimp parameters, of normal and digested tendon. Section 4 shows that a mechanical model [2] of the helix (Section 2) can predict changes in material property from crimp microstructure (Section 3), thus providing biomechanical insight.

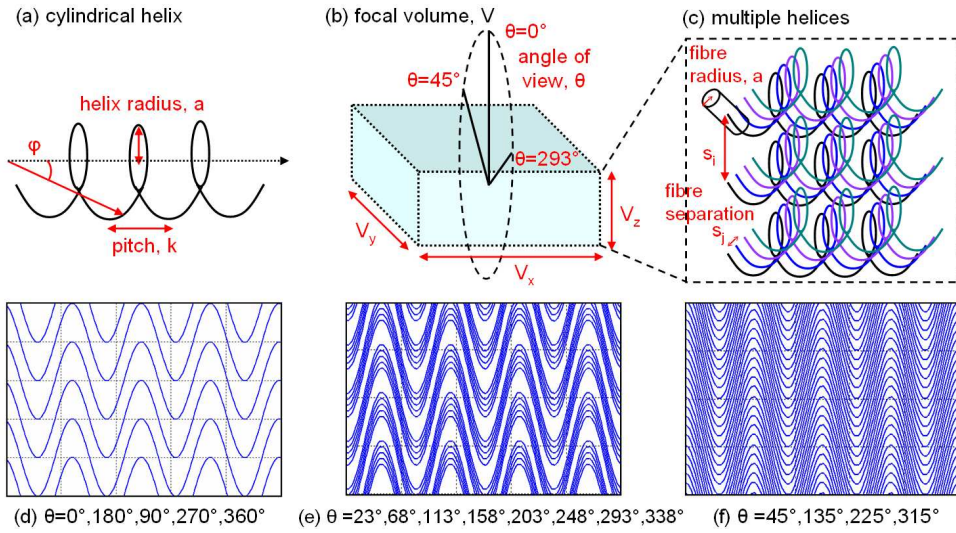


Figure 2: (a) Cylindrical helix model, (b) focal volume illustrating angle of view, and (c) multiple helix model. (d)-(f) Image projections across a range of angles reveal planar crimp.

## 2 Multiple cylindrical helix fibre model

This section proposes a multiple cylindrical helix fibre model which accounts for the experimentally observed rotational invariance, as well as the reported 2D and 3D crimp architectures [2], described in Section 1. Each fibre,  $\mathbf{f}$ , is defined by a helix:

$$\mathbf{f}(\varphi, k, a) = \begin{pmatrix} a \cos \varphi \\ a \sin \varphi \\ k\varphi \end{pmatrix}, \quad (1)$$

where  $a$  is the radius, and  $k$  is the pitch of the helix (Figure 2 (a)).

Our multiple helix model assumes tightly and regularly packed fibres, with fibre separations,  $s_i$  and  $s_j$  (Figure 2 (a)). To investigate crimp architecture, simulated image projections over focal volume slice thickness,  $V_z$ , revealed that a 2D sinusoidal crimp waveform is obtained for a range of angles of view,  $\theta$ , orthogonal to the tendon longitudinal axis (Figures 2 (d)-(f)). Parameters  $k$  and  $a$  determine fibre geometry and thus govern the crimp waveform; the focal volume defines the tissue section being imaged. Future work will investigate variable focal volume, fibre separation and fibre radius,  $r$  (e.g. 50-500 nm [2]).

## 3 Model-fitting to tendon microstructure

This section demonstrates that the model presented in Section 2 can be used to characterise and interpret images of normal and damaged tendon. To experimentally induce tendon damage, bovine flexor tendon samples were incubated in papain enzyme (500  $\mu\text{g}/\text{ml}$ , overnight at 37°C). Control (normal) samples were incubated in phosphate buffered saline. Tendon samples were imaged along the longitudinal axis, using high field (7 T)  $T_1$ -weighted MRI (TR 0.1 s; TE 0.0125 s) and NIR-MPLSM (800 nm excitation; 400 nm SHG emission).

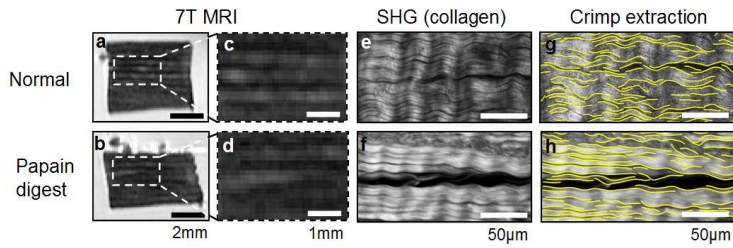


Figure 3: Imaging reveals normal (top) and damaged (bottom) tendon microstructure. (a)-(b) High field MRI, (c)-(d) magnified MRI regions, (e)-(f) SHG images, and (g)-(h) crimp.

High field MRI (Figures 3 (a)-(d)) revealed striations, reflecting fascicle-surrounding tissue (high signal intensity) and intrafascicle regions (low signal intensity). Fascicular integrity and organisation is disrupted by papain digestion (Figure 3 (d)) compared to the normal sample (Figure 3 (c)). The limited resolution of MRI, however, precludes crimp characterisation at this level. For model-fitting, crimp parameters were extracted for SHG images (Figures 3 (e)-(h)), assuming 2D sinusoidal crimp, and using the method provided in [3]. Normal tendon crimp parameters ( $A = 5.12 \pm 1.87 \mu\text{m}$ ;  $\lambda = 32.9 \pm 4.11 \mu\text{m}$ ;  $\psi = 17.3^\circ$ ) were altered by papain digestion ( $A = 2.77 \pm 0.280 \mu\text{m}$ ;  $\lambda = 42.9 \pm 5.68 \mu\text{m}$ ;  $\psi = 7.4^\circ$ ). Model helix radius and pitch are approximated by the crimp wavelength and amplitude, respectively.

## 4 Biomechanical insight

Deriving material properties from images, in particular static images, is challenging. To overcome this challenge, structural information contained in the images, such as fascicular and fibre organisation (*e.g.* crimp), can inform mechanical models (*e.g.* elastic spring [2]), which in turn can be used to obtain material properties. This section shows that the proposed helical model (Section 2) can predict changes in material property from tendon crimp microstructure (Section 3): and simulates mechanical data in agreement with the protective role of fibre crimping [1], preventing tissue damage, in response to nonlinear low strains.

In particular, Freed and Doehring (2005) propose a closed form analytical solution to the mechanical behaviour of a helix [2]. This model predicts increasing stiffness of the nonlinear section of tendon extension with increasing crimp wavelength (amplitude constant, Figure 4 (a)) and decreasing stiffness with increasing amplitude (wavelength constant, Figure 4 (b)). Preliminary results of this model with data from normal and damaged tendon (Section 3 crimp parameters) suggest that nonlinear low strain behaviour in damaged tendon is abbreviated and stiffer than in normal tendon (Figure 4 (c)). Higher stiffness is consistent with earlier entry into the linear deformation regime and hence earlier mechanical failure. Graphs in Figure 4 reflect a realistic nonlinear elastic response of tendon under low strain.

## 5 Discussion

This paper demonstrated that multimodal imaging, high field MRI and NIR-MPLSM, can reveal ECM damage at different levels of the tendon hierarchy. It proposed a multiple cylindrical helix model for interpreting longitudinal tendon SHG images, by predicting changes

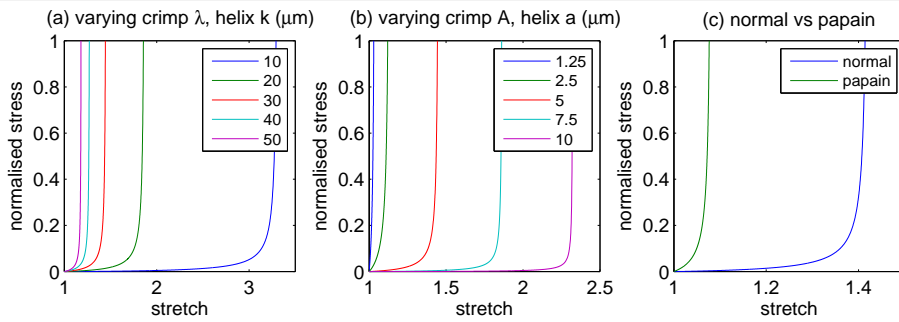


Figure 4: Predicted behaviour of the nonlinear section of tendon extension. (a) Increasing stiffness with increasing crimp wavelength,  $\lambda$ . (b) Decreasing stiffness with increasing crimp amplitude,  $A$ . (c) Papain-digested tendon is stiffer than normal tendon.

in material property and behaviour from tendon crimp microstructure. The multiple helix model is consistent with helical subunits (*e.g.* tropocollagen) at lower hierarchical levels; and comparable to the design of steel wire ropes, which transfer multiaxial heavy loads and adjacent wires compensate for damage *via* friction. In conclusion, this paper demonstrates the clinical potential for assessing tendon using high field MRI, and deriving material properties from intrafascicle regions *via* microscopic endoscopy [5] or biopsy analysis.

**Acknowledgements** The authors would like to thank Philippa Hulley for her advice regarding enzyme digestion, Lowri Cochlin for her help acquiring the MR images, and Uday Tirlapur and Clarence Yapp for their help acquiring the SHG images. Ann K. Harvey is supported by the EPSRC PhD Pilot Plus Scheme (DFDAAA6/15/DD0A6).

## References

- [1] P. Fratzl, K. Misof, I. Zizak, G. Rapp, H. Amenitsch, and S. Bernstorff. Fibrillar structure and mechanical properties of collagen. *J Struct Biol*, 122(1-2):119–22, 1998.
- [2] A. D. Freed and T. C. Doehring. Elastic model for crimped collagen fibrils. *J Biomech Eng*, 127(4):587–93, 2005.
- [3] A.K. Harvey, M. S. Thompson, Z. Cui, and M. Brady. Geometric quantification of tendon second harmonic images. In *MIUA*, pages 259–263, London, 2009.
- [4] P. Kannus. Tendons—a source of major concern in competitive and recreational athletes. *Scand J Med Sci Sports*, 7(2):53–4, 1997.
- [5] J. G. Snedeker, G. Pelled, Y. Zilberman, F. Gerhard, R. Muller, and D. Gazit. Endoscopic cellular microscopy for in vivo biomechanical assessment of tendon function. *J Biomed Opt*, 11(6):064010, 2006.
- [6] T. Szilágyi, A.K. Harvey, M. Brady, L. E. Cochlin, and N. Joshi. Quantitative analysis of tendon ecm damage using mri. In *IEEE ISBI*, Rotterdam, The Netherlands, 2010.
- [7] James H.-C. Wang. Mechanobiology of tendon. *J Biomech*, 39(9):1563–1582, 2006.